Supplementary Information

Synthesis and DFT Study of NH_2-MOF235(Fe)-Derived $ZnFe_2O_4$-Fe_2O_3-ZnO Multiple Heterojunction Nanocomposites for Triethylamine Gas Detection

Hang Zhu[1,2,3], Panpan Li[1], Chengfeng Li[1], Xuanwei Zhao[1], Fanghao Lu[4], Haoyang Sun[1], Tianye Yang[*1,2,3], and Yubin Lan[1,5]

1. National Key Laboratory of Automotive Chassis Integration and Bionics/ School of Mechanical and Aerospace Engineering, Jilin University, Changchun, 130022, People's Republic of China

2. Key Laboratory of CNC Equipment Reliability, Ministry of Education, Jilin University, Changchun, 130022, People's Republic of China

3. Chongqing Research Institute, Jilin University, Chongqing, 400000, China

4. School of Advanced Technology, Xi'an Jiaotong–Liverpool University, Su Zhou, 215123, China

5. School of Agricultural Engineering and Food Science, Shandong University of Technology, Zibo, 255000, China

*Corresponding authors. *E-mail* address: yangty@jlu.edu.cn

1. Material information

All the chemical reagents used in the experiments were purchased and used directly without further purification. Dimethylformamide (DMF, ACS reagent, ≥ 99.8%) and zinc nitrate hexahydrate ($Zn(NO_3)_2·6H_2O$, reagent grade, 98%) were purchased from Sigma Aldrich (Shanghai) Trading Co. Ferric chloride hexahydrate ($FeCl_3·6H_2O$, AR, 99%), 2-aminoterephthalic acid (NH_2-BDC, ＞ 98%), terephthalic acid (PTA, 99%), polyvinylpyrrolidone (PVP, average Mw 58000, K29-32), dimethyl sulfoxide (DMSO, ＞ 98%), and methanol (spectroscopic grade ≥ 99.9%) were purchased from Shanghai Aladdin Ltd. Deionized water (resistivity 18.2 MΩ·cm) was used in all experiment.

All the chemicals used for preparing gases in the subsequent gas sensitivity tests were purchased directly and used without further purification. Formaldehyde (AR, wt% 37.0%~40.0%) was purchased from Liaoning Quanrui Reagent Co., Ltd. Ethanol (AR, wt% ≥ 99.7%) was purchased from Tianjin Fuyu Fine Chemical Co., Ltd. Acetone (AR, ≥ 99.5%) and aniline (AR, wt% ≥ 99.5%) were purchased from Tianjin Yongsheng Fine Chemical Co., Ltd. Triethylamine (AR, ≥ 99.0%) was purchased from Shanghai Aladdin Co.,Ltd. Trimethylamine (AR, 30 wt% in H_2O) was purchased from Shanghai McLean Biochemical Science and Technology Co., Ltd. Ammonia (AR, wt% 25~28%) was purchased from Beijing Chemical Industry Factory.

2. Heterojunction sample synthesis experiment

2.1 Synthesis experiment of NH_2-MOF235(Fe)

Firstly, 50 mL conical flasks were taken out and labeled as A and B. In flask A, 0.55 mmol of ferric chloride hexahydrate and 0.85 mmol of 2-aminoterephthalic acid were dissolved in 15 mL of DMF solution and stirred for 15 minutes. Flask B contained 15 mL of ethanol. After stirring flask A for 15 minutes, the solution from flask A was added dropwise to flask B, and stirring was continued for another 15 minutes. These steps were repeated six times. The six solutions were then transferred into 50 mL PTFE liners and placed in a reactor at 85°C for 12 hours. After the reaction, the samples were allowed to cool naturally to room temperature. The precipitates were collected and washed three times with deionized water and anhydrous ethanol, respectively. Finally, the samples were dried in a constant temperature oven at 60°C for 10 hours, resulting in the synthesis of the Fe-MOF precursor for further preparation.

2.2 Synthesis of $ZnFe_2O_4$-Fe_2O_3-ZnO multi-heterojunction nanocomposites

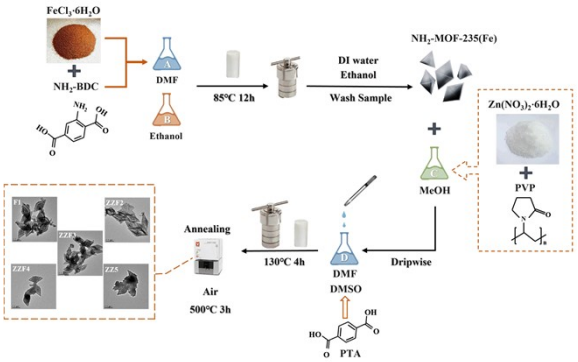

Fig. S1 Schematic of the experimental synthesis of NH_2-MOF235(Fe)@MOF5 MOF-on-MOF derived multiple heterojunction nanocomposites.

0.1g of Fe-MOF precursor, prepared from the above experiments, was dispersed in 10 mL of methanol solution in a conical flask labeled C. The mass of $Zn(NO_3)_2$ added was 0.05, 0.16, 0.25, 0.72, and 1.08 g. The samples were labeled as samples numbered F1, ZZF2, ZZF3, ZZF4, and ZZ5, respectively. To each samples No. F1-ZZ5, 0.1 g of PVP was added and stirred for 15 minutes. Subsequently, five portions of 3.3 mmol of PTA were dissolved in a mixture of 20 mL of DMF and 10 mL of DMSO in a conical flask labeled D and stirred for 15 minutes to obtain five portions of the PTA solution. At the end of stirring, the PTA solution was added dropwise to the F1-ZZ5 sample solution, stirred for 15 min and then kept at room temperature for 45 minutes. Subsequently, the F1-ZZ5 sample solutions were then transferred into 50 mL of PTFE liners and placed in a reactor at 130°C for 4 hours. After the reaction, the samples were cooled naturally to room temperature, the precipitates were collected and washed three times by centrifugation in deionized water and anhydrous ethanol, respectively. After washing, the samples were dried in a constant temperature drying oven. Finally, the products were annealed in a muffle furnace at 500°C for 3 h to obtain samples F1-ZZ5. The experimental synthesis schematic is shown in Fig. S1, thus completing the synthesis of NH_2-MOF235(Fe)@MOF5 MOF-on-MOF derived $ZnFe_2O_4$-Fe_2O_3-ZnO ternary heterojunction nanocomposites.

3. Fabrication of sensors

The sensor consists of a heterojunction material with a ceramic substrate, schematically shown in Fig. S2. The ceramic substrate has a total size of about 1.5×1.5 mm and is made of sintered alumina. The surface of the measuring electrode is plated with gold to increase conductivity. Firstly, an appropriate amount of powdered sample was added the mortar and pestle, assisted by the addition of an appropriate amount of deionized water to form a paste. Pt conductors were soldered to the substrate, and the material was coated onto the inter-finger electrode on the surface of the ceramic substrate.

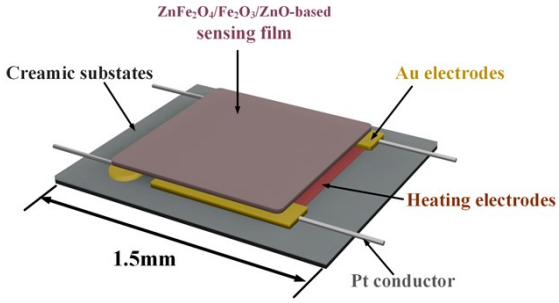

Fig. S2 Schematic diagram of ceramic substrate sensor for gas sensitive test.

4. Material characterization apparatus

XRD data acquisition and material composition analysis of the heterogeneous junction sensing materials was performed using a SHIMADZU LabX XRD-6100 X-ray diffractometer (XRD) with CuKα radiation (λ = 0.154 nm). Raman spectra of the samples were obtained using a Horiba LabRAM HR Evolution instrument to observe the intermolecular vibrations and provide information on the phases and structures of the samples. The micro-scale morphology and structure of the materials, as well as the distribution of elements, were characterized by TESCAN VEGA4 tungsten filament scanning electron microscopy (SEM) and EDS surface scanning. The nanoscale morphology of the samples was observed using a FEI Tecnai F20 transmission electron microscope (TEM) to obtain both TEM and high-resolution transmission electron micrographs (HRTEM). X-ray Photoelectron Spectroscopy (XPS) were obtained using an ESCALAB MKII to visualize the elemental composition and chemical states of the samples. The optical properties and defects of the samples were analyzed by UV-vis spectroscopy with a Hitachi U4150 and photoluminescence (PL) spectroscopy with an Edinburgh FLS1000.

5. SEM of NH_2-MOF235(Fe)

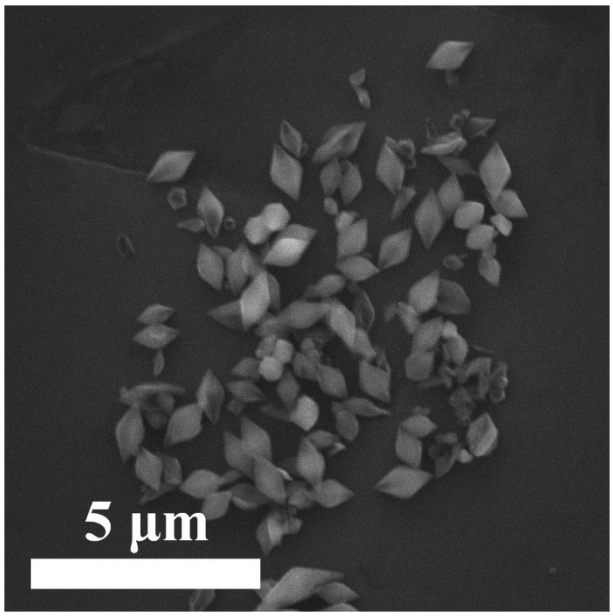

Fig. S3 Polyhedral rhombic SEM of NH_2-MOF235(Fe) without the addition of Zn compounds.

6. Elemental weight (Table S1) and atomic percentages (Table S2) obtained by EDS scanning Mapping

Table S1.

Percentage of weight fraction (wt%) of EDS scanned Fe, Zn, O elements in each sample.

Sample	F1	ZZF2	ZZF3	ZZF4	ZZ5
Fe	69.4 wt%	52.4 wt%	59.3 wt%	13.9 wt%	9.7 wt%
Zn	0.3 wt%	20.0 wt%	12.4 wt%	67.5 wt%	72.6 wt%
O	30.3 wt%	27.6 wt%	28.3 wt%	18.6 wt%	17.7 wt%

Table S2.

Percentage of atomic fractions (at%) of EDS scanned Fe, Zn, O elements in each sample.

Sample	F1	ZZF2	ZZF3	ZZF4	ZZ5
Fe	39.4 at%	31.6 at%	37.0 at%	9.9 at%	7.2 at%
Zn	0.0 at%	10.3 at%	5.9 at%	40.7 at%	46.4 at%
O	60.6 at%	58.1 at%	57.1 at%	49.4 at%	46.4 at%

7. XPS

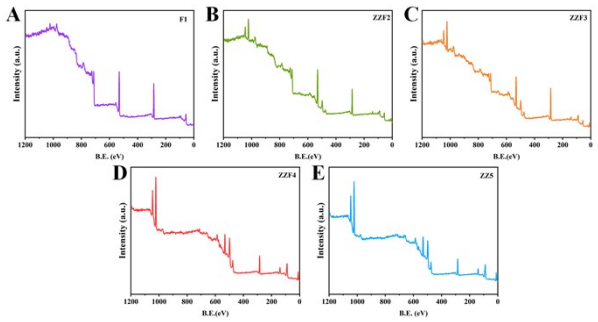

Fig. S4 XPS full test energy spectrum of the sample.

8. DFT calculation details

All first-principles density functional theory (DFT) calculations were conducted using the Vienna Ab-initio Simulation Package (VASP) [1-3]. The Perdew-Burke-Ernzerh (PBE) in the generalized gradient approximation (GGA) with the on-site Coulomb Repulsion U term was applied to describe the exchange-correlation function [4, 5]. In this work, U(Zn)=5.0 eV and U(Fe)= 3.5 eV for all the calculations. Based on the plane wave method, the projector augmented-wave (PAW) method with an energy cutoff of 400 eV was implemented for the electron-ion interactions [6, 7]. The van der Waals interaction was taken into account using DFT-D3 method with Becke-Jonson damping dispersion correction. All structures were fully relaxed until the electronic energy and force acting on atom were smaller than 10^{-4} eV and 0.05 eV·Å^{-1}, respectively. The Brillouin-zone sampling was conducted using Monkhorst-Pack (MP) grids of special points with the separation of 0.04 Å^{-1}. A Gaussian smearing of 0.05 eV was applied to speed up self-consistent field iteration. A vacuum height of >15 Å along the vertical direction was selected to avoid the unwanted interaction between the slab and its period images. The optimized structures were illustrated with VESTA software [8].

8.1 Ball-and-stick structure models

After the original cell models of Fe_2O_3, ZnO, and $ZnFe_2O_4$ surface were established, the structures were optimized, and the crystal faces of different components were matched and optimized. The model of no adsorbed gas was established by matching the (001) face of Fe_2O_3 with the (001) face of ZnO, (111) face of $ZnFe_2O_4$ with the (001) face of Fe_2O_3, (111) face of $ZnFe_2O_4$ with the (001) face of ZnO.

8.2 Details of adsorption energy calculation

The adsorption energy indicates the energy change of the gas molecules during the adsorption

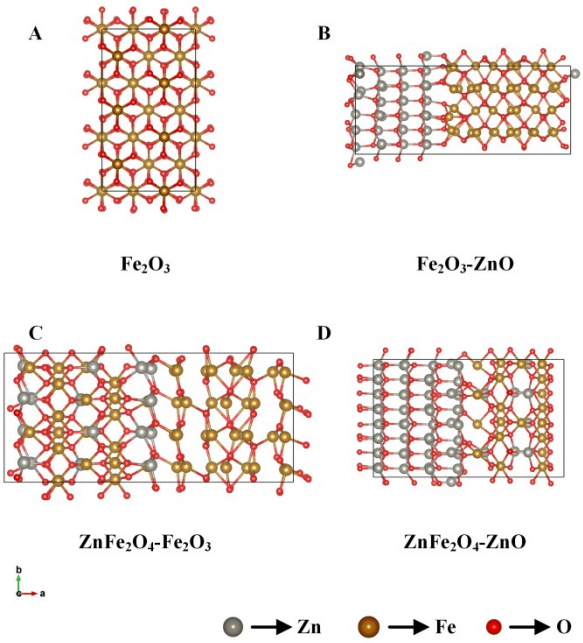

Fig. S5. Structural modeling of Fe_2O_3 and the three types of heterojunctions molecules.

process, which is calculated by Equation S1 [9]. Among them, E_{total} is the total energy of the gas molecules after adsorption on the surface of the material, $E_{surface}$ indicates that it is the energy of the surface of the material, and E_{gas} indicates the energy of the gas molecules.

$$E_{ads} = E_{total} - (E_{surface} + E_{gas}) \quad \text{(S1)}$$

9. Heterogeneous junction gas sensitization mechanism and details of EDL.

The gas-sensitive mechanisms are primarily attributable to the thickness-control model of the surface depletion layer, also known as the grain-boundary barrier model. $ZnFe_2O_4$, Fe_2O_3, and ZnO are n-type semiconductors, where the main carriers are free electrons. The sensitization process and mechanism of multiple heterojunction-based gas sensors is investigated by studying the electronic properties of the multiple heterojunction materials in an atmospheric environment. Redox on the sample surface involves the adsorbed oxygen negative ions reacting with TEA, releasing the trapped electrons back into the material's conduction band. Consequently, the depletion layer is lowered, and the return of free electrons reduces the thickness and height of the potential barriers, resulting in a decrease in the resistance of the material. At higher temperatures, the enhancement of the sensor material's surface activity and the consumption of adsorbed oxygen leads to the transport of oxygen negative ions through the lattice of the material. The lattice oxygen can be directly converted into surface oxygen vacancies by reacting with reducing gases, thereby increasing the material's reactivity.

Multiple heterojunctions can provide a more complex mechanism for the regulation of energy band structure, with the modulation of different ratios of Fe and Zn to form heterojunctions with altered ratios.

References

1. G. Kresse and J. Furthmiiller, Efficiency of ab-initio total energy calculations for metals and semiconductors using a plane-wave basis set, Computational Materials Science, 1996, 6, 36.
2. G. Kresse and J. Furthmüller, Efficient iterative schemes for ab initio total-energy calculations using a plane-wave basis set, PHYSICAL REVIEW B, 1996, 54.
3. G. Kresse and J. Hafner, Ab.initio molecular dynamics for liquid metals, PHYSICAL REVIEW B, 1993, 47.
4. J. P. Perdew, K. Burke and M. Ernzerhof, Generalized Gradient Approximation Made Simple, PHYSICAL REVIEW LETTERS, 1996, 77.
5. J. P. Perdew and Y. Wang, Accurate and simple analytic representation of the electron-gas correlation energy, PHYSICAL REVIEW B, 1992, 45.
6. P. E. Blöchl, Projector augmented-wave method, PHYSICAL REVIEW B, 1994, 50.
7. G. Kresse and D. Joubert, From ultrasoft pseudopotentials to the projector augmented-wave method, 1999, 59.
8. K. Momma and F. Izumi, VESTA 3 for three-dimensional visualization of crystal, volumetric and morphology data, J. Appl. Crystallogr., 2011, 44, 1272-1276.
9. M. Y. Z. Sun, M. S. Chen, X. Y. Cui, Z. M. Zhao, J. H. Wang, L. Liang and Y. T. Zhou, Unveiling the gas sensing potential of C_xN_y monolayer through ab initio screening, Surf. Interfaces, 2023, 42, 8.